cmgh
CELLULAR AND MOLECULAR GASTROENTEROLOGY AND HEPATOLOGY

ORIGINAL RESEARCH

A Novel Gastric Spheroid Co-culture Model Reveals Chemokine-Dependent Recruitment of Human Dendritic Cells to the Gastric Epithelium

Thomas A. Sebrell,[1,*] Marziah Hashimi,[1,*] Barkan Sidar,[2] Royce A. Wilkinson,[1] Liliya Kirpotina,[1] Mark T. Quinn,[1] Zeynep Malkoç,[2] Paul J. Taylor,[3] James N. Wilking,[2] and Diane Bimczok[1]

[1]Department of Microbiology and Immunology, [2]Department of Chemical and Biological Engineering and Center for Biofilm Engineering, Montana State University, Bozeman, Montana; [3]GeneSearch, Inc, Bozeman, Montana

SUMMARY

Human gastric spheroids recruited dendritic cells (DCs) to the basolateral surface of the epithelium through a chemokine-dependent mechanism and established tight contacts with the DCs. *Helicobacter pylori* infection of the organoids increased DC recruitment and enabled DC phagocytosis of the bacteria.

BACKGROUND & AIMS: Gastric dendritic cells (DCs) control the adaptive response to infection with *Helicobacter pylori*, a major risk factor for peptic ulcer disease and gastric cancer. We hypothesize that DC interactions with the gastric epithelium position gastric DCs for uptake of luminal *H pylori* and promote DC responses to epithelial-derived mediators. The aim of this study was to determine whether the gastric epithelium actively recruits DCs using a novel co-culture model of human gastric epithelial spheroids and monocyte-derived DCs.

METHODS: Spheroid cultures of primary gastric epithelial cells were infected with *H pylori* by microinjection. Co-cultures were established by adding human monocyte-derived DCs to the spheroid cultures and were analyzed for DC recruitment and antigen uptake by confocal microscopy. Protein array, gene expression polymerase chain reaction array, and chemotaxis assays were used to identify epithelial-derived chemotactic factors that attract DCs. Data from the co-culture model were confirmed using human gastric tissue samples.

RESULTS: Human monocyte-derived DCs co-cultured with gastric spheroids spontaneously migrated to the gastric epithelium, established tight interactions with the epithelial cells, and phagocytosed luminally applied *H pylori*. DC recruitment was increased upon *H pylori* infection of the spheroids and involved the activity of multiple chemokines including CXCL1, CXCL16, CXCL17, and CCL20. Enhanced chemokine expression and DC recruitment to the gastric epithelium also was observed in *H pylori*–infected human gastric tissue samples.

CONCLUSIONS: Our results indicate that the gastric epithelium actively recruits DCs for immunosurveillance and pathogen sampling through chemokine-dependent mechanisms, with increased recruitment upon active *H pylori* infection. *(Cell Mol Gastroenterol Hepatol 2019;8:157–171; https://doi.org/10.1016/j.jcmgh.2019.02.010)*

Keywords: Stomach; Organoid; Mononuclear Phagocyte; In Vitro Model.

See editorial on page 155.

Infection with the gastric pathogen *Helicobacter pylori* is the leading cause of chronic gastritis, peptic ulcer disease, mucosa-associated lymphoid tissue lymphoma, and gastric adenocarcinoma worldwide.[1,2] Dendritic cells (DCs) in the human gastric mucosa are thought to be the major antigen-presenting cells that induce protective immune responses to *H pylori* infection.[3] We previously showed that human HLA-DR^{high} gastric mononuclear phagocytes (MNPs) with functional properties of DCs were present directly adjacent to the gastric epithelium or integrated within the gastric epithelium.[4] In a mouse model of *Helicobacter* infection, increased numbers of CD11c^{+} DCs migrated to the epithelial layer and extended projections between the gastric epithelial cells.[5] These interactions between DCs and the epithelium likely promote sampling of *H pylori* bacteria from the gastric lumen. Close association with the epithelium also positions the DCs for uptake of *H pylori* antigen that may have crossed the epithelial barrier into the gastric lamina propria. Furthermore, bidirectional cross-talk between gastric mucosal DCs and epithelial cells contributes to the maintenance of gastric homeostasis, as we have shown.[6,7]

A recent study performed in murine small intestine showed that MNP recruitment to the epithelium at steady state is dependent on CCR6 and is required for luminal antigen access.[8] However, the mechanisms that determine how human gastric DCs are recruited and retained by the gastric

*Authors share co-first authorship.

Abbreviations used in this paper: **CagA, cytotoxin-associated antigen; ADC, dendritic cell; FITC, fluorescein isothiocyanate; GFP, green fluorescent protein; IL, interleukin; MNP, mononuclear phagocyte; MoDC, monocyte-derived dendritic cell; RT-PCR, reverse-transcription polymerase chain reaction; TLR, Toll-like receptor.**

Most current article

2352-345X
https://doi.org/10.1016/j.jcmgh.2019.02.010

epithelium currently are unclear. Therefore, we developed an in vitro co-culture model of human gastric spheroids and monocyte-derived DCs (MoDCs) to study the mechanisms of gastric DC–epithelial interactions in primary human cells.

Transwell-based co-culture systems have provided crucial insights into the interactions of the gastrointestinal epithelium with pathogens and immune cells.[9–12] In a groundbreaking study by Rescigno et al,[9] DCs were shown to open the tight junctions between epithelial cells, send dendrites outside the epithelium, and directly sample bacteria from the luminal side of the colonic epithelium. Co-culture studies also have shown the importance of transforming growth factor-β and thymic stromal lymphopoietin for the homeostatic conditioning of intestinal DCs by the epithelium.[10,12] However, traditional co-culture systems have several drawbacks. First, epithelial monolayers for co-culture studies generally are derived from transformed cell lines such as Caco2 cells, which differ in their phenotype and function from primary epithelial cells. Second, epithelial cells in co-culture systems usually are cultured on Transwell inserts composed of a synthetic polymer membrane with pores. This membrane presents an artificial barrier that impairs and limits the contact between immune cells and the epithelium. Third, to promote contacts between DCs and the basolateral side of the epithelium, DCs are either placed on the basolateral side of inverted Transwells, so that they move toward the epithelium because of gravity,[10,13] or epithelial cells are seeded on top of the DCs,[14] also leading to forced interactions.

In 2 recent studies, researchers have started to use organoids as an improved epithelial cell model to investigate epithelial interactions with immune cells.[15,16] Our co-culture model of human gastric epithelial spheroids and MoDCs lead to the spontaneous establishment of direct interactions between DCs and the basolateral side of the gastric epithelium. By using this model, we showed that DCs added to gastric epithelial spheroid cultures spontaneously migrated toward the epithelium to establish tight contacts. DC migration was dependent on epithelial chemokine secretion and was enhanced in the presence of luminal *H pylori* infection. Moreover, DCs were able to phagocytose *H pylori* applied to the spheroid lumen. These functionally relevant findings indicate that our primary cell co-culture model is suitable for studies of gastric infection and epithelial–immune cell interactions and will allow us to advance our understanding of human gastric immunobiology.

Results

Human DC Are Recruited to the Epithelium of Gastric Spheroids

To perform functional studies of human DC interactions with the gastric epithelium, we generated gastric epithelial spheroids from adult stomach tissue and then established co-cultures with human DCs by adding immature MoDCs to the culture medium surrounding the epithelial spheroids (Figure 1*A*). Although DCs appeared to accumulate at the

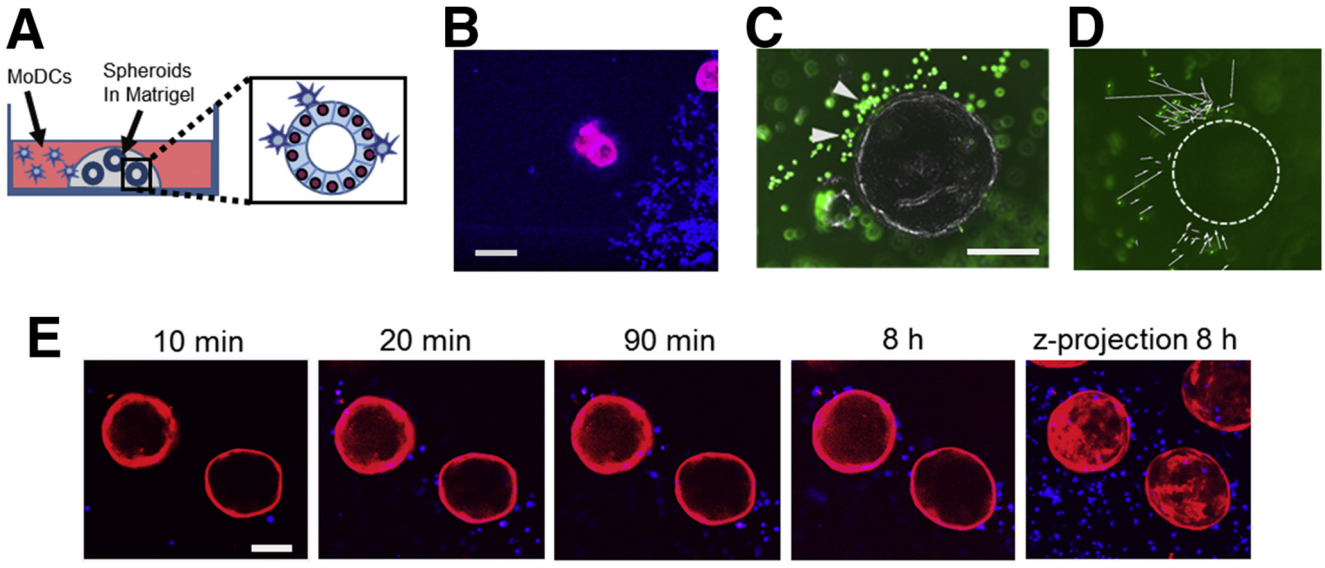

Figure 1. MoDCs spontaneously migrate to the basolateral side of the gastric epithelium upon co-culture with gastric spheroids. (*A*) Graphic representation of the DC–epithelial spheroid co-culture model. (*B*) Fluorescent confocal image of the bottom of a representative culture plate shows the Matrigel border with accumulated cells. Blue, CellTracker DeepRed-labeled DCs; red, mCherry-expressing spheroids. *Scale bar*: 200 μm. (*C*) Representative gastric spheroid with surrounding CellTracker Green-labeled MoDCs. Merge of phase-contrast image and green fluorescent image. *Arrowheads* indicate accumulated MoDCs. *Scale bar*: 200 μm. (*D*) Particle tracking analysis of time-lapse images shows DC tracks directed toward the spheroid. *Dotted line* indicates the position of the spheroid. Images were acquired on an EVOS FL Auto system with a 10$\times$ objective and are representative of 4 independent experiments. (*E*) Time-lapse confocal imaging of mCherry-expressing gastric spheroids and CellTracker DeepRed-labeled MoDCs (blue) shows rapid recruitment of MoDCs to the spheroids. Single images obtained at different time points after initiation of the co-culture and a Z-stack projection of 50 slices obtained after 8 hours (*right*, step size 10 μm). *Scale bar*: 100 μm. All data are representative of 4 or more independent experiments performed with different spheroid lines and DC preparations.

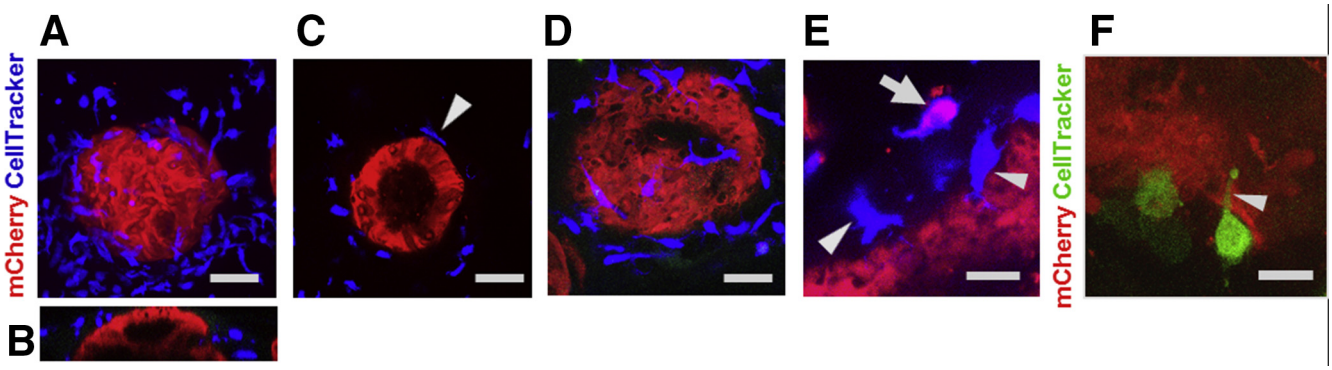

Figure 2. MoDCs directly associate with the epithelium of co-cultured gastric spheroids. CellTracker-labeled MoDCs were added to cultures of mCherry-expressing gastric spheroids. After 48 hours, cultures were fixed and imaged on a Leica SP5 Confocal Scanning Laser Microscope using a 63× water immersion objective. (*A–C*) CellTracker DeepRed-labeled MoDCs (blue) that have migrated to the basolateral side of a gastric epithelial spheroid (red). *Scale bar*: 50 μm. (*A*) XY image, maximum Z projection of 57 individual images, step size of 1 μm. (*B*) XZ projection of the same spheroid. (*C*) Single XY slice shows the physical association between a DC (*arrowhead*) and the spheroid. (*D*) Z-projection of 6 adjacent slices shows extensive dendrite formation on the surface of a gastric spheroid. (*E*) High-resolution image showing CellTracker DeepRed-labeled MoDCs (blue) in direct contact with gastric epithelial cells (*arrowheads*) and 1 MoDC with internalized mCherry$^+$ gastric epithelial cell material (pink in merged image; *arrow*). Single XY slice. *Scale bar*: 20 μm. (*F*) CellTracker Green-labeled MoDC (green) extending a dendrite (*arrowhead*) into the epithelial layer (red). XY image, Z projection of 4 adjacent slices. *Scale bar*: 20 μm. All data are representative of 4 or more independent experiments performed with different spheroid lines and DC preparations.

border between the tissue culture medium and the spheroid-containing Matrigel plug to some extent (Figure 1*B*), a considerable number of DCs rapidly entered the Matrigel matrix and associated with the organoids. Live imaging of spheroids and CellTracker Green-labeled (ThermoFisher Scientific, Waltham, MA) MoDCs showed that DCs spontaneously migrated toward the epithelium of the spheroids and accumulated around the basolateral side of the gastric epithelium (Figure 1*C* and Supplementary Video). Importantly, particle tracking analysis showed directed migration of the DCs toward the basolateral side of the epithelial cells (Figure 1*D*). In fact, some gastric spheroid–associated DCs were detected as early as 10 minutes after initiation of the experiment (Figure 1*E*).

MoDCs Establish Direct Contacts With Co-cultured Gastric Epithelial Spheroids

To analyze the interactions between human gastric epithelial spheroids and co-cultured DCs in more detail, we performed high-resolution confocal imaging of co-cultures. DCs frequently were present directly adjacent to the basolateral side of the epithelium (Figure 2*A–C*). Specifically, MoDCs formed direct contacts with the epithelium and extended long dendrites along the basolateral side of the gastric epithelium (Figure 2*D–F*). In some instances, dendrites with globular endings were extended between the epithelial cells (Figure 2*F*). These dendrites were morphologically similar to the transepithelial dendrites formed by DCs in the stomach and intestine in vivo and in other co-culture systems.[5,9,15,17,18] Notably, some MoDCs contained mCherry-positive cytoplasmic inclusions (Figure 2*E*), possibly representing phagocytosed material derived from apoptotic gastric epithelium.[7] Interestingly, we also detected DCs that had migrated into the spheroid lumen in 7 of 159 (4.4%) spheroids analyzed (data not shown). Overall, these observations indicate that DCs in our co-culture model spontaneously establish interactions with the gastric epithelium.

H pylori *Infection of Human Gastric Epithelial Spheroids Induced Increased Recruitment of DCs to the Gastric Epithelium*

To determine the effects of luminal *H pylori* infection on DC recruitment to the spheroid epithelium, we performed microinjection of gastric spheroids with *H pylori*. Successful injections were confirmed by replating a small proportion of dissociated spheroids at the end of the experiment. Recovery of significant numbers of viable bacteria was achieved consistently after 48 hours, but bacterial numbers varied widely between experiments (Figure 3*A*). In contrast, *H pylori* were unable to survive when injected directly into Matrigel, (Corning, Corning, NY) and we also were unable to recover viable bacteria from the media surrounding the injected organoids (not shown). Interestingly, bacterial recovery was decreased in cultures where DCs were present than in cultures of infected organoids alone (Figure 3*A*). Luminal oxygen concentrations in the gastric spheroids were reduced significantly compared with the surrounding Matrigel, possibly supporting growth of the microaerophilic *H pylori* (Figure 3*B*). These data are consistent with earlier reports showing that human intestinal organoids have reduced luminal oxygen levels.[19]

We next performed confocal imaging analysis of DCs co-cultured with green fluorescent protein (GFP)–*H pylori*–infected or mock-injected gastric spheroids (Figure 3*D*). DCs were added 2–3 hours after *H pylori* infection of the spheroids. After 48 hours, a significantly higher number of DCs was detected in close proximity to *H pylori*–infected spheroids compared with noninfected spheroids (Figure 3*C* and *E*). We also compared DC

recruitment by gastric spheroids injected with *H pylori* 60190 with DC recruitment by spheroids injected with the Toll-like receptor (TLR)5 agonist *Salmonella* flagellin, which consistently induced spheroid activation as determined based on *CXCL8* gene expression (Figure 3*F*). Fluorescein isothiocyanate (FITC) dextran was injected as a fluorescent tracer to identify injected organoids that remained intact throughout the experiment. TLR stimulation caused a slight, but not significant, increase in DC recruitment (Figure 3*G*). Interestingly, however, infection of the organoids with a cytotoxin-associated antigen A (CagA)-negative deletion mutant of *H pylori* 60190[20] did not enhance DC accumulation above baseline (Figure 3*G*). Intensity analysis of FITC-dextran fluorescence showed no difference between treatments, indicating that the injected substances did not significantly alter epithelial barrier function (data not shown). Overall, these observations suggest that *H pylori* infection promotes DC recruitment to the gastric epithelium, likely through a mechanism that involves *H pylori*–dependent release of chemotactic factors by the epithelial cells.

Gastric Epithelial-Derived Chemokines Induce DC Recruitment

To determine the mechanism for DC recruitment to the gastric epithelium, we analyzed supernatants from gastric

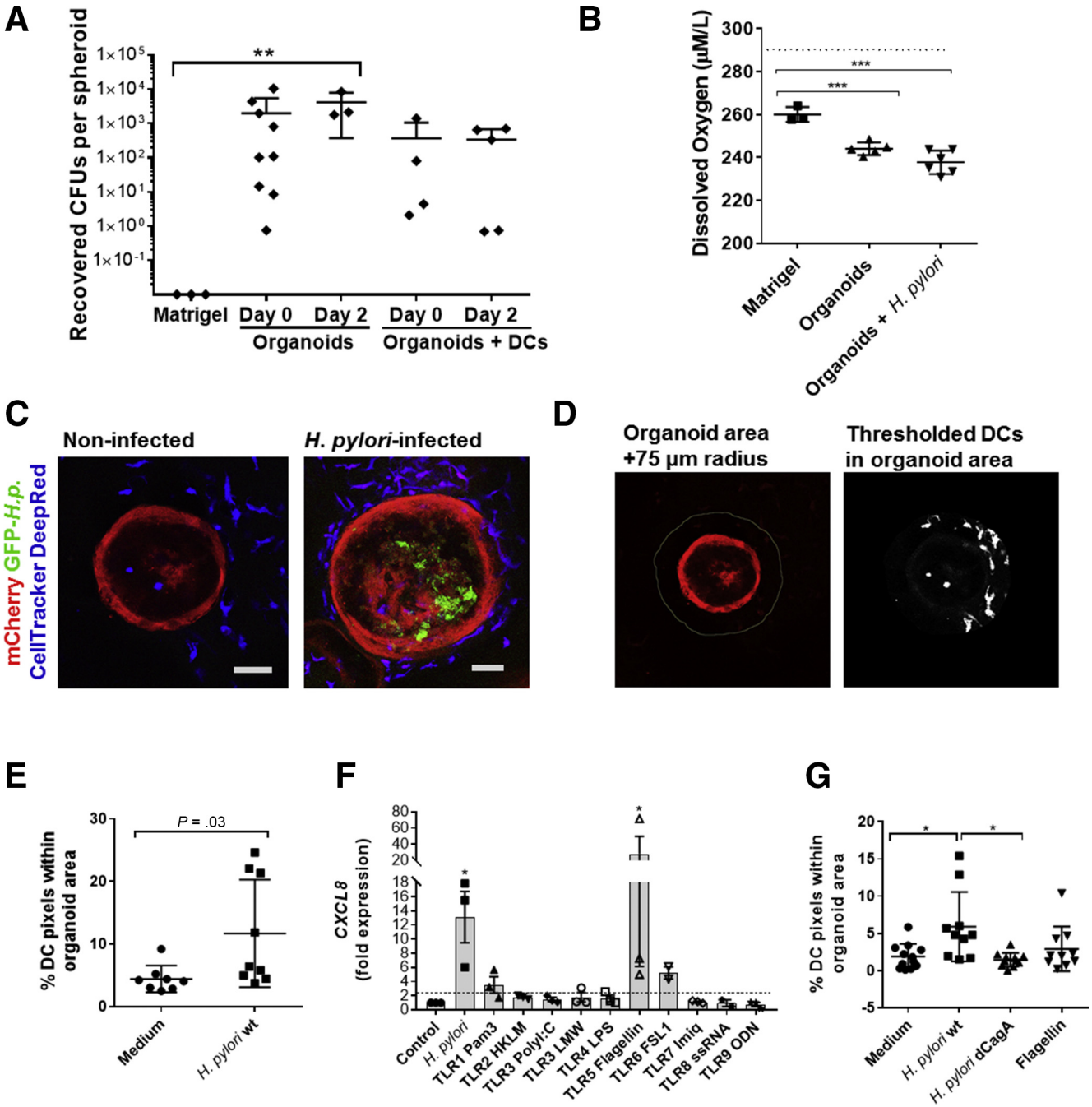

spheroid cultures in Transwell chemotaxis assays. MoDCs were significantly recruited by supernatants from uninfected spheroid supernatants (Figure 4*A*), consistent with the data obtained by microscopic analysis of the MoDC–gastric spheroid co-cultures. Moreover, *H pylori* infection of the spheroids significantly increased the chemotactic index of MoDCs toward spheroid culture supernatants (Figure 4*B*), corroborating the confocal microscopy data shown in Figure 3. Notably, we did not observe significant chemokinetic activity of MoDCs in response to gastric spheroid supernatants (data not shown). Addition of pertussis toxin (10 μg/mL), which blocks G-protein–dependent signaling, significantly reduced DC recruitment by both *H pylori*–infected and noninfected spheroids, suggesting that DC recruitment is mediated by chemokine-dependent mechanisms (Figure 4*C*).

To identify the chemokines involved in both steady-state and infection-induced recruitment of DCs to the gastric epithelium, we performed a chemokine antibody array with supernatants from noninfected and *H pylori*–infected gastric spheroids. By using this approach, we detected baseline secretion of CXCL5, CXCL17, CCL20, CXCL8 (interleukin [IL] 8), CXCL16, CXCL1, and midkine (neurite growth-promoting factor 2) $\geq$2-fold greater than background levels present in spheroid media, with considerable variations between spheroid lines (Figure 4*D* and Supplementary Table 1). Spheroid infection with *H pylori* significantly increased secretion of CCL20 and consistently up-regulated CXCL1 and CXCL8 by the gastric epithelium, whereas CXCL16, CXCL17, and midkine consistently were decreased in the presence of *H pylori.*

We also analyzed the effect of *H pylori* infection of human gastric spheroids on chemokine gene expression using an RT^2 Profiler (Qiagen, Valencia, CA) reverse-transcription polymerase chain reaction (RT-PCR) gene expression array (Figure 4*E* and Supplementary Table 2). Overall, gene expression patterns largely matched protein secretion data. *CXCL1*, *CXCL2*, and *CXCL8* were up-regulated significantly after 3 hours of *H pylori* stimulation in 3 independent experiments ($P \leq .05$), confirming results from previous studies.[21,22] *CCL2*, *CCL20*, *CXCL3*, and *CXCL6* also were up-regulated consistently by $\geq$2-fold in *H pylori*–infected spheroids, but the magnitude of up-regulation varied widely. No significant down-regulation was observed for any of the genes analyzed.

Having shown that luminal application of wild-type *H pylori* but not of CagA-deficient *H pylori* or *Salmonella* flagellin induced an accumulation of DCs immediately around the organoid (Figure 3*G*), we next compared the chemotactic activity and the chemokine profile of supernatants recovered from spheroids treated with broth alone, wild-type *H pylori*, CagA-deficient *H pylori*, and flagellin. Similar to our observations with the co-cultures, wild-type *H pylori* was the most efficient at inducing DC chemotaxis ($P \leq .01$), but the CagA-deficient *H pylori* also induced significant DC migration in the Transwell assay ($P \leq .05$), whereas no significant effects were observed for flagellin application (Figure 4*F*). Analysis of chemokines in the culture supernatants showed inconsistent changes in the chemokine profiles between the different treatment groups (Figure 4*G*). Chemokines induced by the CagA-deficient *H pylori* largely followed the same pattern as those induced by wild-type *H pylori*, with similar CCL20 and CXCL1 release, but significantly lower CXCL8 levels. In contrast, flagellin caused higher CXCL8 release, but lower CCL20 release compared with wild-type *H pylori*. These observations suggest that a combination of redundantly active chemokines control DC recruitment to the gastric epithelium.

Human MoDCs Show Chemotactic Responses to CXCL1, CXCL16, CXCL17, and CCL20

Having shown that gastric spheroids release factors with chemotactic activity for human DCs and that multiple chemokines, including CXCL5, CXCL17, CCL20, CXCL8, CXCL16, CXCL1, are released basolaterally by gastric spheroids, we

Figure 3. (*See previous page*). *H pylori* infection of human gastric epithelial spheroids leads to increased DC recruitment. (*A*) Bacterial recovery from Matrigel alone or from *H pylori*–infected gastric spheroids (20–50/culture) with or without co-cultured MoDCs present. Spheroid cultures were disrupted by trypsinization within the first 3 hours after *H pylori* infection or 48 hours later, and cells were plated for colony-forming unit (CFU) counts (N = 3–9). Means ± SD and individual values are shown. $^{**}P \leq .01$, Kruskal–Wallis test with the Dunn multiple comparison. (*B*) Microsensor analysis of luminal oxygen concentrations measured in gastric spheroids (n = 5 or 6 organoids, means ± SD). $^{***}P \leq .001$, 1-way analysis of variance with the Dunnett multiple comparison. *Dotted line* indicates the concentration of oxygen in buffer. (*C*) Representative confocal images (single optical sections) of a noninfected and a GFP–*H pylori* (green)-infected, mCherry-expressing gastric spheroid (red) co-cultured with CellTracker-labeled MoDCs (blue) for 48 hours. *Scale bar*: 50 μm. (*D*) Image analysis approach for organoid co-cultures. The organoid area was defined as the area within a 75-μm radius of the spheroid, and the DC area was measured digitally on an auto-thresholded image. (*E*) Digital image analysis of 8 noninfected and 9 spheroid co-cultures infected with GFP–*H pylori* from 3 independent experiments. Individual data points, means ± SD are shown. Significance between groups was analyzed by an unpaired Student *t* test. (*F*) Gastric epithelial spheroids were replated as monolayers and treated with *H pylori* 60190 wild type (wt, 5 × 10^7/well) or a panel of TLR agonists (see the Materials and Methods section) for 6 hours. Gene expression of *CXCL8* was determined by quantitative RT-PCR. Individual values (*symbols*) and means ± SD (*bar* and *error bars*) from 3 independent experiments are shown. $^{*}P \leq .05$; Kruskal–Wallis test with the Dunnett multiple comparison. (*G*) Gastric spheroids were microinjected with FITC dextran alone (molecular weight, 4 kilodaltons, tracer) or with FITC dextran containing *H pylori* 60190 wild type, *H pylori* 60190 ΔCagA, or *Salmonella* flagellin (1 μg/mL). Spheroids that remained intact throughout the experiment, as determined by retention of FITC dextran in the lumen, were analyzed for DC recruitment after 48 hours. Pooled data from 2 independent experiments were analyzed by Kruskal–Wallis test with the Dunn multiple comparison ($^{*}P \leq .05$). All co-cultures were imaged on a Leica SP5 Confocal Scanning Laser Microscope using a 20× objective, and imaging data were analyzed using ImageJ software.

tested the ability of human MoDCs to migrate toward these chemokines (Figure 5). In Transwell chemotaxis assays, the DCs showed a strong and significant response to CXCL1 and CXCL16 (Figure 5*E* and *F*) and a moderate response to CCL20 and CXCL17 (Figure 5*C* and *E*). A weak chemotactic response was observed to CXCL5 and CXCL8 (Figure 5*A* and

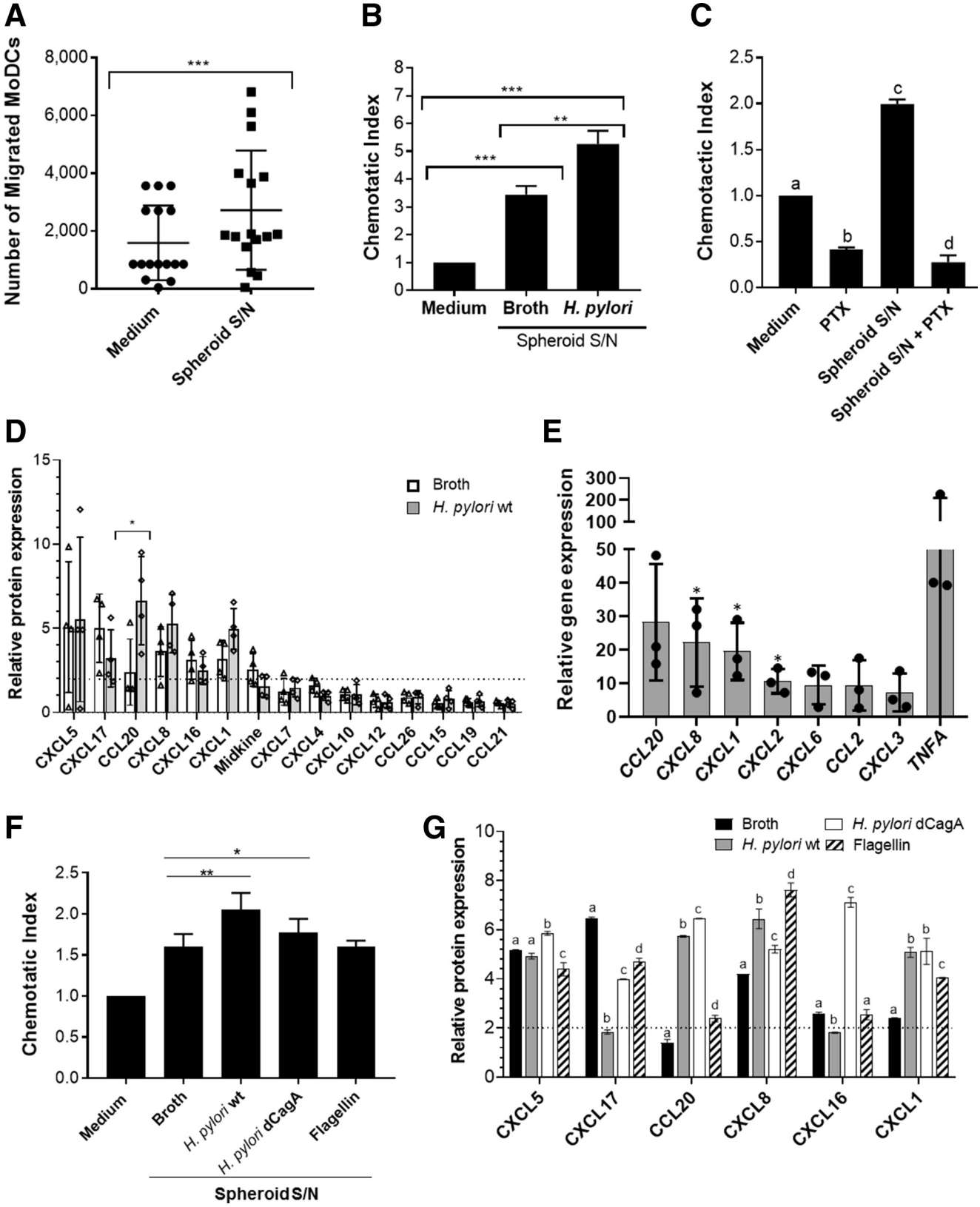

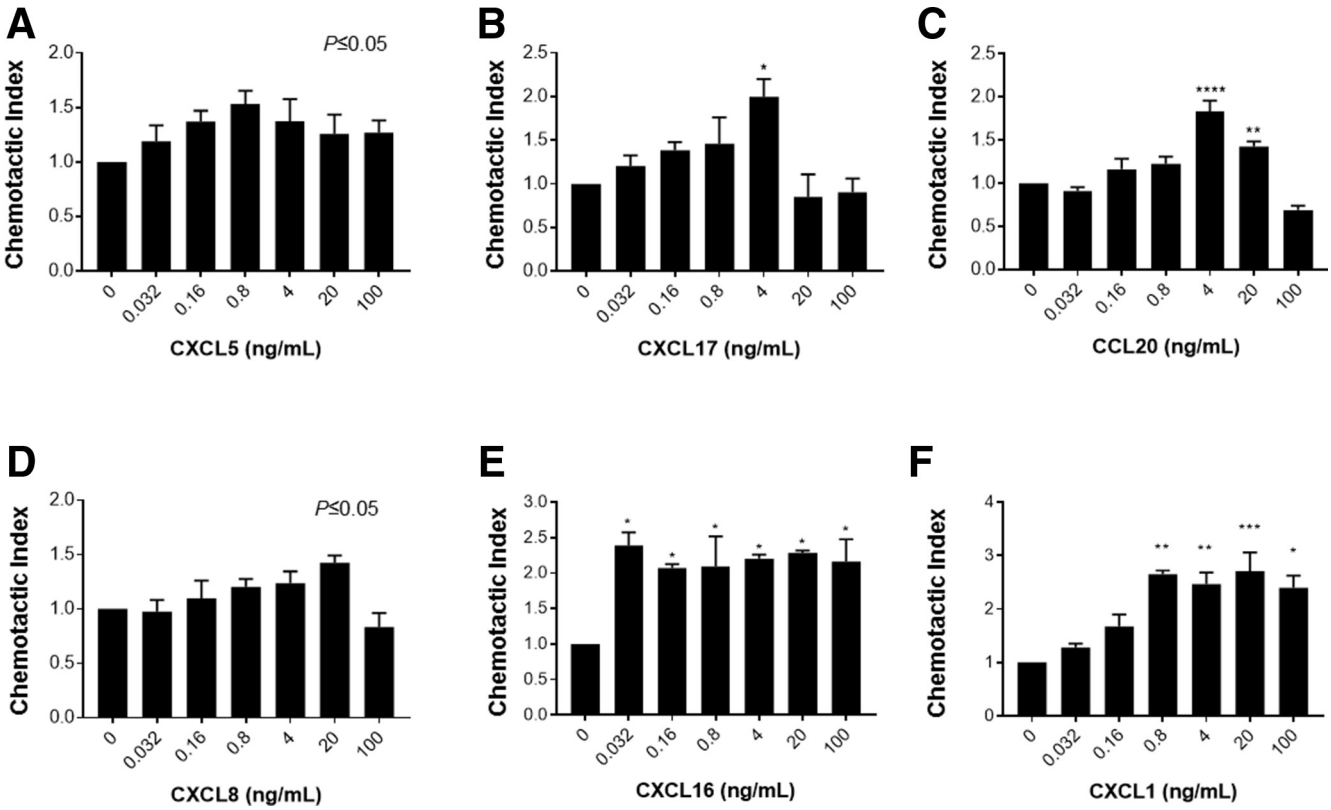

Figure 5. MoDCs show chemotactic activity to multiple chemokines that are released by the gastric epithelium. Chemotactic activity of MoDCs toward various concentrations of (*A*) CXCL5, (*B*) CXCL17, (*C*) CCL20, (*D*) CXCL8, (*E*) CXCL16, and (*F*) CXCL1 was analyzed in Transwell chemotaxis assays. Representative results of 3 or more experiments each are shown. Means ± SD of triplicate wells, analyzed by 1-way analysis of variance. The Tukey post hoc test was used to determine differences between individual chemokine concentrations and control, *$P \leq .05$, **$P \leq .01$, ***$P \leq .001$, and ****$P \leq .0001$.

D). Together with the observations shown in Figure 4, these data indicate that DC recruitment to the epithelial interface involves the activity of multiple epithelial-derived chemokines and that *H pylori* infection increases the immune cell recruitment to the epithelium by up-regulating chemokine expression.

Human H pylori *Infection Increases Chemokine Expression and DC Recruitment to the Epithelium*

To confirm the relevance of our in vitro data, we analyzed chemokine gene expression and epithelial DC recruitment in gastric tissues from *H pylori*–infected and

Figure 4. (***See previous page***). ***H pylori* infection increases human gastric epithelial cell chemokine expression, leading to enhanced DC recruitment.** (*A*) Culture supernatants (S/Ns) collected over 48 hours from established spheroid cultures were tested for their ability to attract MoDCs (2×10^5/well) in a Transwell chemotaxis assay. Individual data points from 16 independent experiments performed in triplicate (means ± SD, ***$P \leq .001$, paired Student *t* test). (*B*) Culture supernatants collected from gastric spheroids with or without *H pylori* infection 48 hours after microinjection of the spheroids were analyzed in Transwell chemotaxis assays with MoDCs (1×10^5/well). Means ± SD of triplicate wells, 1 representative experiment out of 4 is shown. Analysis of variance with the Tukey multiple comparisons test (**$P \leq .01$, ***$P \leq .001$). (*C*) MoDC chemotaxis to medium alone or gastric spheroid supernatants in the presence of absence of pertussis toxin (PTX, 10 μg/mL) was analyzed. Means ± SD of triplicate wells, 1 representative experiment out of 3 is shown. Analysis of variance with the Tukey multiple comparison test; different letters signify statistically significant differences ($P \leq .05$). (*D*) Supernatants collected from spheroid cultures with and without *H pylori* infection (48 h) were analyzed for the presence of chemokines using a chemokine array. Pooled data from 4 independent experiments. *$P \leq .05$, Student *t* test. (*E*) Relative gene expression of select chemokine and cytokine genes in *H pylori*–infected compared with noninfected spheroids. Means ± SD of 3 independent infection experiments. Only genes that showed consistent >2-fold up-regulation in all 3 experiments are shown. *$P \leq .05$, Student *t* test. (*F*) Culture supernatants were collected after 48 hours from gastric spheroids microinjected with broth alone, *H pylori* wild type (wt), *H pylori* ΔCagA, or *Salmonella* flagellin. Supernatants were analyzed in Transwell chemotaxis assays with MoDCs. One representative experiment out of 3 is shown, means ± SD of triplicate wells, analysis of variance with the Tukey multiple comparison test; *$P \leq .05$, **$P \leq .01$. (*G*) Supernatants from spheroid cultures with different treatments were analyzed for the presence of chemokines by chemokine array. One representative experiment out of 2 is shown. Different letters signify statistically significant differences in chemokine concentration ($P \leq .05$).

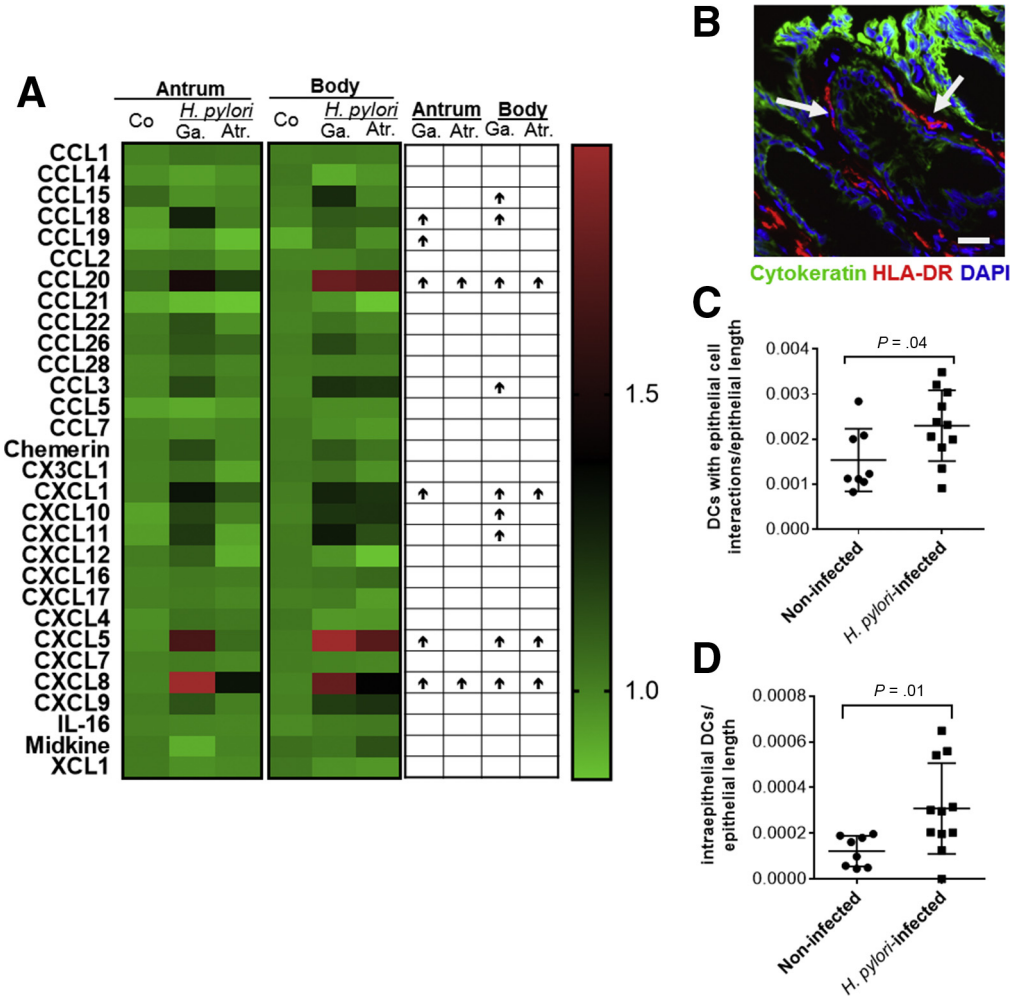

Figure 6. *H pylori* infection induces increased chemokine expression in gastric tissues and enhances the recruitment of DCs to the gastric epithelium. (*A*) Heatmap showing relative chemokine gene expression in human gastric antrum and body from noninfected (Co) and *H pylori*–infected donors without atrophy (gastritis, Ga) and with gastric atrophy (Atr) (n = 3 each). Data were extracted from Gene Expression Omnibus data set records GDS5338 (antrum) and GDS5411 (body). *Arrow* indicates significant up-regulation (analysis of variance with the Dunnett multiple comparisons test, $P \leq .05$). (*B–D*) Gastric biopsy samples from *H pylori*–infected (n = 11) and noninfected (n = 8) human donors were immunolabeled for HLA-DR (Cy3, red) and epithelial cytokeratin (type 7/8; FITC, green). Cell nuclei were labeled with 4′,6-diamidino-2-phenylindole (DAPI) (blue). Images were acquired on a Nikon Eclipse T2000-U fluorescent microscope equipped with a CoolSnap ES digital camera and NIS Elements BR2.30 software with a 20× objective. (*B*) Representative image of non–*H pylori*–infected mucosa. *Arrows* indicate examples of DCs in direct contact with epithelial cells. *Scale bar*: 20 μm. (*C*) The number of HLA-DR^{high} DCs in direct contact with the basal side of the gastric epithelium was counted and normalized to epithelial length. Data from individual subjects, means ± SD, are shown. Data were analyzed by the Student *t* test. (*D*) The number of intraepithelial DCs was determined using the approach described for panel *C*.

noninfected donors. Gene expression profiling data overall were consistent with protein and gene expression data obtained from gastric spheroids (Figure 6*A*). *CCL20*, *CXCL1*, *CXCL5*, and *CXCL8* were up-regulated significantly ($P \leq .05$) in the *H pylori*–infected gastric body with and without atrophy and in the *H pylori*–infected gastric antrum without atrophy, and *CCL20* and *CXCL8* expression remained significantly increased in atrophic gastric antrum. We also detected significantly up-regulated expression of several other chemokines such as *CCL18* and *CXCL10*, predominantly in nonatrophic samples from the gastric body. In contrast, *H pylori* infection did not alter the gene expression of *CXCL17* and *CXCL16* in any of the groups.

We next analyzed whether human *H pylori* infection increases DC recruitment to the gastric epithelium in situ. As previously shown, DCs in the gastric mucosa frequently interact with the epithelium (Figure 6*B*). Importantly, the number of both lamina propria DCs in direct contact with the gastric epithelium and the number of intraepithelial DCs was increased significantly in *H pylori*–infected samples (Figure 6*C* and *D*) ($P = .04$ and $P = .01$, respectively).

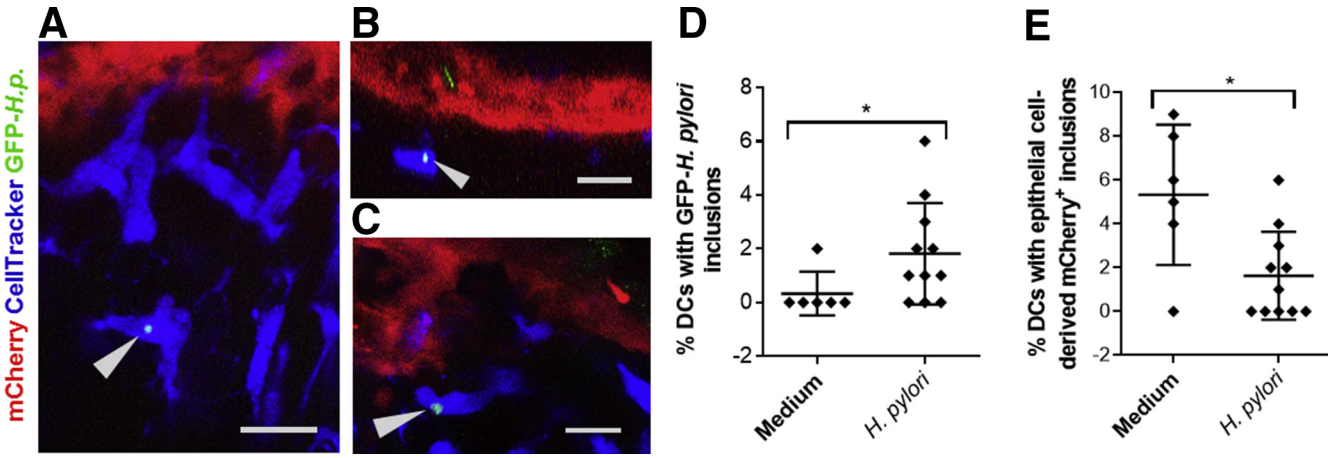

Figure 7. MoDCs co-cultured with *H pylori*–infected human gastric spheroids phagocytose *H pylori* bacteria. (*A–C*) Confocal image analysis of gastric epithelial spheroid–MoDC co-cultures show internalized GFP-positive material in a subset of MoDCs (*arrowheads*). mCherry-expressing spheroids (red) were infected with GFP–*H pylori* (green), and CellTracker-labeled MoDCs (blue) were added for 48 hours. Representative images of 3 independent co-culture experiments. *Scale bar*: 20 μm. (*D* and *E*) Percentage of MoDCs with (*D*) green fluorescent (GFP^+) inclusions and (*E*) red fluorescent ($mCherry^+$) inclusions (see Figure 3*E*, pink in merged images) after 48 hours of co-culture with noninfected vs GFP–*H pylori*–infected gastric spheroids. Co-cultures were imaged on a Leica SP5 Confocal Scanning Laser Microscope using a 63× objective. Data from 1 of 3 representative experiments; individual data points, means and SD, are shown. *$P \leq .05$, Mann–Whitney *U* test.

Co-culture of MoDCs With H pylori*–Infected Gastric Epithelial Spheroids Results in DC Uptake of* H pylori

To determine whether DC-epithelial interactions in gastric spheroid-DC co-cultures enable the DCs to sample *H pylori* antigens, we used high-resolution confocal imaging. A significant percentage of MoDCs in *H pylori*–infected co-cultures (1.8% ± 0.6%) contained GFP-positive material consistent with phagocytic uptake of *H pylori* ($P \leq .05$), whereas green fluorescent material generally was absent from DCs in co-cultures that were not infected with GFP–*H pylori* (Figure 7*A–D*). Interestingly, 5.3% ± 1.3% of DCs in spheroid co-cultures contained CellTracker-labeled material of presumed epithelial origin (Figure 7*E*), as shown in Figure 2*E*. The proportion of these cells was decreased significantly upon *H pylori* infection ($P \leq .05$). Overall, these results suggest that MoDCs co-cultured with gastric spheroids perform relevant phagocytic functions, as shown for mononuclear phagocytes in gastric tissues.[7,23]

Discussion

The immunologic mechanisms specific to the human stomach as a unique mucosal environment remain poorly understood. Specifically, it is unclear how antigen-presenting cells are recruited to and interact with the gastric epithelium to access *H pylori* antigens. To address this knowledge gap, we have developed and evaluated a novel organotypic co-culture model based on primary human cells that enables functional studies of the interactions between the gastric epithelium, DCs, and luminal *H pylori* bacteria. With this model, we show that human DCs show chemotactic activity for epithelial-derived factors and form tight interactions with the epithelium. Importantly, *H pylori* infection of the gastric epithelium increased epithelial chemokine expression and DC recruitment to the epithelial interface, both in our co-culture model and in *H pylori*–infected human subjects.

Cross-talk between MNP populations and epithelial cells at mucosal sites is important for immunosurveillance and mucosal imprinting of the MNPs by epithelial-derived factors.[6,24,25] In our model, MoDCs co-cultured with gastric epithelial spheroids spontaneously migrated toward the gastric epithelium and established direct contacts with the epithelial cells. To establish contacts with the epithelium, the MoDCs actively penetrated the Matrigel within less than 30 minutes. DCs have been shown previously to migrate through Matrigel by using matrix metalloproteinases that degrade extracellular matrix components.[26,27] Once DCs have migrated toward the gastric epithelium, our co-cultures closely resembled the human gastric mucosa, where MNPs are present immediately beneath the epithelial cell layer and sometimes integrated into the epithelium.[4,7,17] Moreover, the MoDCs extended dendrites between epithelial cells that were morphologically similar to those previously reported to be involved in antigen uptake by MNPs in the small intestine[18,28] and the stomach.[5,17] It is possible that the dendrites seen in our model enabled the observed phagocytosis of GFP–*H pylori* bacteria in our study.

Notably, DCs were recruited to the epithelium in the absence of inflammation or infection, likely representing steady-state recruitment. Because of the short life span of mucosal DCs, constant DC recruitment is necessary to replace dying cells to maintain epithelial immunosurveillance.[29] A similar steady-state recruitment of DCs to the epithelium recently was shown in the murine intestine.[8] Importantly, we also showed that DC recruitment to the epithelial interface was increased upon *H pylori* infection,

both in our co-culture model and in gastric biopsy specimens obtained from human donors. Our study thus confirms and extends previous reports that *H pylori* infection induces gastric epithelial chemokine expression and significantly promotes MNP recruitment.[4,5,30,31] In the gastric mucosa, murine *Helicobacter* infection resulted in increased numbers of $CD11c^+$ and $CD68^+$ cells,[5,30,31] and we previously have detected increased numbers of $HLA\text{-}DR^{high}$ MNPs upon human *H pylori* infection.[4] Here, we specifically showed that increased numbers of gastric DCs interacted with the epithelial layer upon *H pylori* infection. These increased interactions may have important functional implications for continuous luminal antigen sampling and for positioning DCs for antigen uptake when the epithelial barrier is compromised during *H pylori* infection. Indeed, DCs co-cultured with *H pylori*–infected spheroids showed evidence of *H pylori* phagocytosis, again resembling the behavior of DCs in *H pylori*–infected gastric mucosa, where *H pylori* phagocytosis by gastric DCs recently was observed in a mouse model.[23]

Interestingly, significantly higher numbers of DCs accumulated at the epithelium of spheroids infected with wild-type *H pylori* compared with CagA-deficient *H pylori*. CagA is a major virulence factor of *H pylori* that is injected into host cells through a type 4 secretion system and that activates a number of proinflammatory host signaling pathways including nuclear factor-κB, leading to enhanced chemokine secretion.[32,33] However, we did not see any clear differences in chemotactic activity of DCs toward supernatants from spheroids infected with wild-type vs CagA-deficient *H pylori.* Although CXCL8 secretion by spheroids infected with CagA-deficient *H pylori* was lower than that induced by wild-type bacteria, confirming earlier studies,[34] other chemokines with stronger chemotactic activity for DCs were unchanged or up-regulated. Thus, the mechanism for the lack of DC recruitment in spheroid co-cultures infected with CagA-deficient *H pylori* remains elusive. Mustapha et al[35] previously investigated *H pylori*–dependent chemokine release using primary gastric epithelial cells and showed that disruption of the CagA type IV secretion system (T4SS) significantly decreased chemokine gene expression after 3 hours, but not after 24 hours. Early differences in chemokine secretion may have contributed to altered DC recruitment toward infected spheroids because co-cultures were established 2–3 hours after injection, but these differences may have disappeared after 48 hours when spheroid supernatants were collected.

By using a combination of chemokine analysis in gastric spheroid supernatants, gene expression profiling of gastric spheroids, DC chemotaxis assays, and gene expression analysis of human gastric tissues, we identified a number of chemokines that likely contribute to DC recruitment to the gastric epithelium under steady-state conditions and during *H pylori* infection. CCL20 was identified as a chemokine that attracted DCs and that was expressed by the gastric epithelium both at steady state and at increased levels upon *H pylori* infection. CCL20 has been shown previously to regulate steady-state DC recruitment to the epithelium in the murine small intestine.[8] However, whether CCL20 promotes recruitment of human DCs has been a matter of debate.[36,37] Here, we show that certain concentrations of CCL20 significantly promoted DC recruitment and therefore may contribute to both steady-state and infection-induced DC recruitment in the stomach. Likewise, CXCL1 was secreted at high levels by the gastric epithelium at steady state, was up-regulated during *H pylori* infection at the protein and the RNA levels, and had significant chemotactic activity on human MoDCs. Thus, CXCL1 likely plays an important role in DC recruitment to the gastric epithelium. CXCL8 is a signature chemokine that activates CXCR2 for neutrophil recruitment and that is known to be up-regulated upon gastric *H pylori* infection.[38,39] We showed that CXCL8 was secreted at a high levels by noninfected gastric spheroids, was up-regulated upon *H pylori* infection in a CagA-dependent manner, and that CXCL8 also acts on DCs. Interestingly, we also showed that gastric epithelial cells release significant amounts of CXCL5, CXCL16, and CXCL17, and that human DCs show chemotactic responses to both chemokines. However, *H pylori* infection increased neither CXCL16 nor CXCL17, suggesting that CXCL16 and CXCL17 play a role in steady-state DC recruitment. Previous studies had shown that activated DCs express CXCL16,[40] but whether human DCs express the CXCL16-receptor CXCR6 and are responsive to CXCL16 has not yet been investigated. Likewise, how DCs respond to CXCL17 is currently unknown because the receptor for this orphan chemokine has not yet been identified.[41]

Taken together, these observations suggest that steady-state migration of DCs to the gastric epithelium involves CXCL1, CXCL5, CXCL8, CXCL16, CXCL17, and CCL20, whereas increased DC recruitment upon *H pylori* infection is driven mostly by CXCL1, CCL20, and possibly CXCL8. Notably, it is unknown whether gastric DCs show chemotactic responses to the same chemokines as the MoDCs used in this study, and we were unable to perform chemotaxis experiments with human gastric DCs owing to limited cell availability. However, we found that chemokine expression by gastric spheroids matched gene expression profiles detected in biopsy specimens of *H pylori*–infected human subjects, and DC recruitment to the epithelium likewise was increased both in our in vitro model and in vivo. These observations indicate that the results obtained with the spheroid-MoDC co-cultures were biologically relevant.

Notably, our model system used organoid cultures of primary human gastric epithelial cells together with human DCs to study gastric immunobiology. A recent study by Noel et al[15] used epithelial monolayers derived from human enteroids and showed that co-cultured macrophages enhanced epithelial barrier function. We previously co-cultured human blood monocytes on the luminal surface of short-term primary gastric epithelial cell cultures to show that human MNPs are conditioned by retinoic acid released by the gastric epithelium.[6] However, unlike retinoic acid, most epithelial surface proteins and soluble mediators are expressed in a polar manner,[15] so that DCs need to be added to the basolateral side of the epithelium to replicate the physiological orientation of the tissue. Most previous studies have used Transwell systems, in which epithelial cells are

seeded on top of a porous membrane and DCs are added to the bottom compartment to achieve the correct spatial relationship between epithelium and immune cells.[9–13,15,42–44] Organoids, including epithelial spheroids and other 3-dimensional long-term culture systems of primary epithelial cells, have a closed lumen and a fully accessible basolateral side on the outside. Thus, our model allows spontaneous interactions between DCs that are added to the cultures and the basolateral surface of the gastric epithelium in the absence of filter membranes. In a similar model, Nozaki et al[16] recently co-cultured murine intraepithelial lymphocytes with small intestinal organoids and showed that dynamic interactions between intraepithelial lymphocytes and the epithelium supported prolonged maintenance of the intraepithelial lymphocytes in culture. Overall, our co-culture system has the advantage of using primary human gastric epithelial cells, allowing direct access of immune cells to the basolateral side of the epithelium, and supporting active *H pylori* infection over several days, and therefore is suitable for studying gastric epithelial cell–DC cross-talk in vitro. Moreover, we anticipate that the DC-epithelial cell co-culture model described here can be easily adapted for studying other mucosal sites, immune cells, and pathogens.

We recognize that our new co-culture system still has certain limitations. Spheroids and organoids occasionally may rupture, releasing luminal material including infectious agents and apoptotic epithelial cell material and mucus in an uncontrolled manner.[45] We addressed this issue by injecting FITC dextran as a tracer into the spheroids. FITC dextran is rapidly released from the spheroid lumen upon rupture, as we have shown.[45] Therefore, organoids that remained intact throughout the experiment could be identified based on the presence of the tracer. However, we still cannot rule out the presence of some *H pylori* bacteria outside the gastric spheroids owing to leakage during microinjection. One other limitation of any organoid culture system is that, unless cells are re-seeded on a Transwell insert, it is impossible to determine epithelial cell numbers, and thus multiplicity of infection, with a high degree of accuracy, owing to differences in size and shape of the organoids. Moreover, bacterial delivery into the lumen of gastric spheroids by microinjection remains difficult to automate. Despite these challenges, our co-culture system yielded reproducible and statistically significant results. Specifically, our experiments using gastric spheroid–MoDC co-cultures have shown that the gastric epithelium promotes accelerated recruitment of DCs to the epithelial cell interface upon *H pylori* infection through a chemokine-dependent mechanism.

Materials and Methods

Human Blood and Tissue Samples

Blood samples for isolation of monocytes were obtained with local Institutional Review Board approval from our healthy adult donor pool at Montana State University by a trained phlebotomist. Healthy human gastric tissue samples for the generation of spheroid lines were obtained with Institutional Review Board approval as surgical resection material from sleeve gastrectomies from the National Disease Research Interchange (Philadelphia, PA).

Gastric Epithelial Spheroid Cultures

Gastric epithelial spheroids were derived from human gastric glands and cultured in the presence of Wnt3a, noggin, and R-spondin, as previously described.[45] Lentiviral transduction was used to generate mCherry-expressing spheroid lines.[45]

MoDCs

$CD14^+$ monocytes were isolated from peripheral blood mononuclear cells using anti-human CD14 MACS beads (130-050-201; Miltenyi Biotec, Cologne, Germany), as previously described.[46] All monocyte preparations were analyzed for activation based on cluster formation and spontaneous tumor necrosis factor-α release, and pre-activated cells were excluded from our experiments. Monocytes then were cultured in RPMI1640 medium supplemented with 10% human AB serum (35060CI; Corning, Manassas, VA), 100 U/L penicillin, 100 μg/L streptomycin (15140-122; Gibco, Waltham, MA), 50 μg/mL gentamycin (IB2030; IBI Scientific, Peosta, IA), 5 mmol/L HEPES (SH3023710), and 2 mmol/L L-glutamine (SH30034.1) (both Hyclone, Logan, UT), 25 ng/mL recombinant human (rh) granulocyte-macrophage colony-stimulating factor (GM-CSF) (215-GM-050), and 7 ng/mL rhIL-4 (204-IL-050) (both R&D Systems, Minneapolis, MN). After 5–6 days in culture, DCs were harvested by vigorous pipetting.

Gastric Epithelial Spheroid–DC Co-cultures

To perform fluorescence imaging, co-cultures were set up using mCherry-expressing spheroid cultures and MoDCs stained with CellTracker Green (C7025) or CellTracker DeepRed (C34565). To establish DC-spheroid co-cultures, spheroid culture medium was replaced with antibiotic-free DC culture medium (RPMI1640 with 10% human AB serum). For each 35-mm MatTek (Ashland, MA) culture plate containing approximately 80 spheroids, we then added 5×10^5 immature MoDCs directly to the medium, overlaying the spheroids in the Matrigel.

Chemokine Detection

To analyze chemokine secretion by gastric spheroids, supernatants were collected from 24-well plates 48 hours after medium change. Supernatants then were analyzed using the Proteome Profiler Human Chemokine Array Kit (ARY017; R&D Systems), which detects 31 different chemokines with specific monoclonal antibodies. Arrays were imaged on a FluorChem R System (Proteinsimple, San Jose, CA), and relative pixel densities of duplicate spots were measured using ImageJ software (National Institutes of Health, Bethesda, MD). Relative chemokine expression was calculated by normalizing results from spheroid supernatants to results obtained with spheroid growth medium alone.

Chemotaxis Assays

The chemotactic activity of MoDCs to spheroid supernatants and recombinant chemokines was measured in a Transwell migration assay using the 96-well ChemoTX system with a 5-μm polycarbonate membrane (106-5; Neuro Probe, Inc, Gaithersburg, MD). MoDCs ($1–2 \times 10^5$) were incubated in triplicate for 4 hours at 37°C, and viable migrated cells were counted using a CellTiter-Glo Luminescent Cell Viability Assay (G7570; Promega, Madison, WI). Migration toward the following recombinant human chemokines was assessed: CXCL1 (300-11), CXCL5 (300-22), CXCL16 (300-55), CCL20 (300-29A, all from PeproTech, Rocky Hill, NJ), CXCL8 (208-IL; R&D Systems), and CXCL17 (NBPS-35133; Novus Biologicals, Littleton, CO). The chemotactic index for recombinant chemokines was calculated by dividing the number of migrated cells for the experimental condition by the number of migrated cells in medium alone. Data from gastric spheroid supernatants were additionally normalized to the number of epithelial cells present in the cultures, as determined by cell counting at the end of the experiment.

H pylori *Infection and TLR Agonist Treatment of Gastric Epithelial Spheroids*

To establish *H pylori* infection of the spheroids, we plated *H pylori* strain 60190 wild type, a CagA-deficient mutant of strain 60190[20] (kind gifts from Dr G. Perez-Perez) or the GFP-expressing strain M6 (a kind gift from Dr John Y. Kao) under microaerophilic conditions on Brucella agar, 5% horse blood (221261; Becton Dickinson) for 3–4 days. Spheroids for injection experiments were seeded on 35-mm MatTek dishes for 8–12 days, with the Matrigel applied as a thin streak to facilitate injection of multiple spheroids. Before injections, gastric epithelial spheroids were overlaid with antibiotic-free medium (3 media changes) for 3 days to prevent bacterial death. We selected spheroids with a diameter of 200–800 μm and used a GeneSearch Embryo Cradle micromanipulator (GeneSearch, Inc, Bozeman, MT) and a 2-μL syringe (Hamilton Co, Reno, NV) for microinjection. Injection needles with beveled tips were pulled from glass capillaries to a tip size of 21-23 μm. We injected 20–80 organoids per culture with 0.2 μL of *H pylori* suspension (2×10^5 bacteria) in Brucella broth, corresponding to a multiplicity of infection of 10–50, or with 1 μg/mL of *Salmonella* flagellin. Control spheroids were injected with Brucella broth alone. In some experiments, 0.2 μL of 25 μmol/L 4 kilodaltons FITC dextran (46944; Sigma-Aldrich, St. Louis, MO) was added to the injection media as a fluorescent tracer. Successful *H pylori* infection was confirmed by re-culturing bacteria recovered from trypsinized organoids on Brucella agar plates and performing colony counts. MoDCs were added to *H pylori*–infected spheroids after 2–3 hours. To evaluate gastric epithelial cell responses to TLR agonist treatment, spheroids were replated on collagen-coated 24-well plates (08-772-71, Biocoat; Corning, Tewksbury, MA). Established monolayers were stimulated for 6 hours with the human TLR1–9 agonist kit containing the following: TLR1/2 agonist: palmitoyl-3-cystein (Pam3CSK4); TLR2 agonist: heat-killed *Listeria monocytogenes* (HKLM); TLR3 agonist: polyinosine-polycytidylic acid (poly(I:C)); TLR3 agonist: poly(I:C)-low molecular weight (LMW); TLR4 agonist: lipopolysaccharide *E coli* K12; TLR5 agonist: flagellin *Salmonella typhimurium*; TLR6/2 agonist: fibroblast-stimulating factor 1 (FSL1); TLR7 agonist: imiquimod; TLR8 agonist: ssRNA40/LyoVec; and TLR9 agonist: oligodeoxynucleotide (ODN)2006 (tlrl-kit1hw; InVivoGen, San Diego, CA), and then were analyzed for *IL8/CXCL8* gene expression using quantitative RT-PCR, as previously described.[47]

Oxygen Concentrations in Gastric Spheroids

Mock-injected spheroids were compared with spheroids infected with *H pylori* bacteria for 3 hours. Oxygen concentration profiles in the organoids were measured with an OX-25 Clark-type oxygen microelectrode with a 25-μm sensor tip diameter (Unisense A/S, Aarhus, Denmark). The microelectrode was connected to a Unisense microsensor multimeter and millivolt data were logged onto a laptop computer with Sensor Trace Pro software (Unisense). A motor-controlled micromanipulator (model MM33; Unisense) was used to move the oxygen electrode during profile measurements. A 2-point calibration was performed for O_2 sensors using buffer sparged with air and medium sparged with pure N_2(g) for at least 30 minutes. An S80 APO stereomicroscope (Leica, Wetzlar, Germany) was used to visualize the microsensor tip and confirm placement on the organoid surface before profiling.

RT^2 *Profiler PCR Array*

To analyze the expression of chemokines, chemokine receptors, and other related genes, we used the Human Chemokines & Receptors RT^2 Profiler PCR array (PAHS-022Z; Qiagen, Valencia, CA), following the manufacturer's instructions. RNA from *H pylori*–infected (strain 60190) or control cultures was isolated using the Direct-zol MiniRNA prep kit (R2052; Zymo Research, Irvine, CA), and 0.15–0.5 μg of RNA was converted into complementary DNA. Arrays were run on a Lightcycler 96 (Roche, Penzberg, Germany) and were analyzed using the Qiagen Data Analysis Center online tool (www.qiagen.com), with a cycle threshold (Ct) cut-off of 35 and β2-microglobulin and *RPLP0* used as housekeeping genes.

Immunofluorescence Analysis of Tissue Sections

Cryosections or a paraffin-embedded gastric tissue microarray[7] (kind gift from Dr Paul Harris, Pontifical Catholic University of Chile, Santiago, Chile) prepared from human gastric tissue were labeled with anti–HLA-DR (cryosections: L243, BD 340689; tissue array: LN-3, ab166777; Abcam, Cambridge, UK) to stain DCs and with anticytokeratin FITC (cryosections: CAM5.2, BD 347653; tissue array: C11; 4545; Cell Signaling Technology, Danvers, MA) to stain epithelial cells, as previously described.[4,7] Cell nuclei were stained with 4′,6-diamidino-2-phenylindole. Samples were imaged on a Nikon Eclipse T2000-U fluorescent microscope (Nikon, Melville, NY) equipped with a CoolSnap ES digital camera and NIS Elements BR2.30 (Nikon). ImageJ V1.48[48] was used to

measure epithelial cell length and count DCs that were in direct contact with the epithelium.

Microscopy and Image Analysis

Epifluorescence and phase-contrast images were acquired on a Nikon Eclipse T2000-U fluorescent microscope equipped with a CoolSnap ES digital camera and NIS Elements BR2.30 software or on a Life Technologies (Carlsbad, CA) EVOS FL Auto system equipped with an onstage incubator. For confocal image analysis, we fixed the co-cultures with Cytofix Reagent (554655; BD Biosciences). Samples were imaged on an inverted SP5 Confocal Scanning Laser Microscope (Leica) with 405-, 488-, 561-, and 633-nm laser excitation lines using a 20× objective or a 63× water immersion objective with Immersol (W 2010; Zeiss, Oberkochen, Germany). We recorded Z-stacks of 2–11 randomly selected organoids with intact morphology for each experiment and experimental conditions. To quantitate MoDC recruitment to the epithelial interface, we used ImageJ version 1.48V,[48] with the LOCI plugin to allow access to Leica .lif files. For analysis of DC recruitment, area and circumference of the spheroid were measured, and pixels positive for the DC dye CellTracker DeepRed (pseudocolored blue) were counted automatically on thresholded images. DCs that were within 75 μm of the basolateral side of the epithelium were considered epithelial cell–associated DCs. To determine MoDC uptake of *H pylori* bacteria or epithelial cell–derived material, DCs with fluorescent inclusions were counted manually on individual confocal slices using the Cell Counter plugin, and the total number of DCs in an image stack was determined by counting the cells on a maximum Z-projection of the image stack.

Live Imaging Analysis and Particle Tracking

Live imaging was performed using a Life Technologies EVOS FL Auto system equipped with an onstage incubator. Fluorescence and phase-contrast images were collected at 10-minute intervals over 48 hours using a 10× objective. The migration of cells toward gastric spheroids was analyzed using the Particle Tracking feature in Imaris version 8.4 (Bitplane, Zurich, Switzerland).

Gene Expression Analysis of Gastric Biopsy Specimens

Gene expression of relevant chemokines in gastric antral and corpus biopsy specimens of non–*H pylori*–infected patients and *H pylori*–infected patients with and without gastric atrophy (n = 3 each) was analyzed using the Gene Expression Omnibus reference series GSE27411 and data set records GDS5411 (body) and GDS 5338 (antrum).[49]

Data and Statistical Analysis

All authors had access to the data and have reviewed and approved the final manuscript. Data were analyzed using GraphPad Prism 7.02 (San Diego, CA). Results are presented as means ± SD. Differences between values were analyzed for statistical significance by the 2-tailed Student *t* test, 1- or 2-way analysis of variance, or the Kruskal–Wallis test with appropriate post hoc tests. Differences were considered significant at $P < .05$.

References

1. Delahay RM, Rugge M. Pathogenesis of Helicobacter pylori infection. Helicobacter 2012;17(Suppl 1):9–15.
2. Cover TL, Blaser MJ. Helicobacter pylori in health and disease. Gastroenterology 2009;136:1863–1873.
3. Shiu J, Blanchard TG. Dendritic cell function in the host response to Helicobacter pylori infection of the gastric mucosa. Pathog Dis 2013;67:46–53.
4. Bimczok D, Clements RH, Waites KB, Novak L, Eckhoff DE, Mannon PJ, Smith PD, Smythies LE. Human primary gastric dendritic cells induce a Th1 response to H. pylori. Mucosal Immunol 2010;3:260–269.
5. Kao JY, Zhang M, Miller MJ, Mills JC, Wang B, Liu M, Eaton KA, Zou W, Berndt BE, Cole TS, Takeuchi T, Owyang SY, Luther J. Helicobacter pylori immune escape is mediated by dendritic cell-induced Treg skewing and Th17 suppression in mice. Gastroenterology 2010;138:1046–1054.
6. Bimczok D, Kao JY, Zhang M, Cochrun S, Mannon P, Peter S, Wilcox CM, Monkemuller KE, Harris PR, Grams JM, Stahl RD, Smith PD, Smythies LE. Human gastric epithelial cells contribute to gastric immune regulation by providing retinoic acid to dendritic cells. Mucosal Immunol 2015;8:533–544.
7. Bimczok D, Smythies LE, Waites KB, Grams JM, Stahl RD, Mannon PJ, Peter S, Wilcox CM, Harris PR, Das S, Ernst PB, Smith PD. Helicobacter pylori infection inhibits phagocyte clearance of apoptotic gastric epithelial cells. J Immunol 2013;190:6626–6634.
8. McDonald KG, Wheeler LW, McDole JR, Joerger S, Gustafsson JK, Kulkarni DH, Knoop KA, Williams IR, Miller MJ, Newberry RD. CCR6 promotes steady state intestinal mononuclear phagocyte association with the intestinal epithelium, imprinting, and immune surveillance. Immunology 2017;152:613–627.
9. Rescigno M, Urbano M, Valzasina B, Francolini M, Rotta G, Bonasio R, Granucci F, Kraehenbuhl JP, Ricciardi-Castagnoli P. Dendritic cells express tight junction proteins and penetrate gut epithelial monolayers to sample bacteria. Nat Immunol 2001;2:361–367.
10. Butler M, Ng CY, van Heel DA, Lombardi G, Lechler R, Playford RJ, Ghosh S. Modulation of dendritic cell phenotype and function in an in vitro model of the intestinal epithelium. Eur J Immunol 2006;36:864–874.
11. Bermudez-Brito M, Munoz-Quezada S, Gomez-Llorente C, Matencio E, Romero F, Gil A. Lactobacillus paracasei CNCM I-4034 and its culture supernatant modulate Salmonella-induced inflammation in a novel Transwell co-culture of human intestinal-like dendritic and Caco-2 cells. BMC Microbiol 2015;15:79.
12. Zeuthen LH, Fink LN, Frokiaer H. Epithelial cells prime the immune response to an array of gut-derived commensals towards a tolerogenic phenotype through distinct actions of thymic stromal lymphopoietin and transforming growth factor-beta. Immunology 2008;123:197–208.

13. Emami CN, Mittal R, Wang L, Ford HR, Prasadarao NV. Recruitment of dendritic cells is responsible for intestinal epithelial damage in the pathogenesis of necrotizing enterocolitis by Cronobacter sakazakii. J Immunol 2011; 186:7067–7079.
14. Leonard F, Collnot EM, Lehr CM. A three-dimensional coculture of enterocytes, monocytes and dendritic cells to model inflamed intestinal mucosa in vitro. Mol Pharm 2010;7:2103–2119.
15. Noel G, Baetz NW, Staab JF, Donowitz M, Kovbasnjuk O, Pasetti MF, Zachos NC. A primary human macrophage-enteroid co-culture model to investigate mucosal gut physiology and host-pathogen interactions. Sci Rep 2017;7:45270.
16. Nozaki K, Mochizuki W, Matsumoto Y, Matsumoto T, Fukuda M, Mizutani T, Watanabe M, Nakamura T. Co-culture with intestinal epithelial organoids allows efficient expansion and motility analysis of intraepithelial lymphocytes. J Gastroenterol 2016;51:206–213.
17. Necchi V, Manca R, Ricci V, Solcia E. Evidence for transepithelial dendritic cells in human H. pylori active gastritis. Helicobacter 2009;14:208–222.
18. Niess JH, Brand S, Gu X, Landsman L, Jung S, McCormick BA, Vyas JM, Boes M, Ploegh HL, Fox JG, Littman DR, Reinecker HC. CX3CR1-mediated dendritic cell access to the intestinal lumen and bacterial clearance. Science 2005;307:254–258.
19. Hill DR, Huang S, Nagy MS, Yadagiri VK, Fields C, Mukherjee D, Bons B, Dedhia PH, Chin AM, Tsai YH, Thodla S, Schmidt TM, Walk S, Young VB, Spence JR. Bacterial colonization stimulates a complex physiological response in the immature human intestinal epithelium. Elife 2017;6.
20. Tummuru MK, Cover TL, Blaser MJ. Mutation of the cytotoxin-associated cagA gene does not affect the vacuolating cytotoxin activity of Helicobacter pylori. Infect.Immun 1994;62:2609–2613.
21. Bartfeld S, Bayram T, van de Wetering M, Huch M, Begthel H, Kujala P, Vries R, Peters PJ, Clevers H. In vitro expansion of human gastric epithelial stem cells and their responses to bacterial infection. Gastroenterology 2015; 148:126–136.
22. Schlaermann P, Toelle B, Berger H, Schmidt SC, Glanemann M, Ordemann J, Bartfeld S, Mollenkopf HJ, Meyer TF. A novel human gastric primary cell culture system for modelling Helicobacter pylori infection in vitro. Gut 2016;65:202–213.
23. Arnold IC, Zhang X, Urban S, Artola-Boran M, Manz MG, Ottemann KM, Muller A. NLRP3 Controls the development of gastrointestinal CD11b(+) dendritic cells in the steady state and during chronic bacterial infection. Cell Rep 2017;21:3860–3872.
24. Iliev ID, Mileti E, Matteoli G, Chieppa M, Rescigno M. Intestinal epithelial cells promote colitis-protective regulatory T-cell differentiation through dendritic cell conditioning. Mucosal Immunol 2009;2:340–350.
25. Iliev ID, Spadoni I, Mileti E, Matteoli G, Sonzogni A, Sampietro GM, Foschi D, Caprioli F, Viale G, Rescigno M. Human intestinal epithelial cells promote the differentiation of tolerogenic dendritic cells. Gut 2009;58:1481–1489.
26. Adhikary S, Kocieda VP, Yen JH, Tuma RF, Ganea D. Signaling through cannabinoid receptor 2 suppresses murine dendritic cell migration by inhibiting matrix metalloproteinase 9 expression. Blood 2012;120:3741–3749.
27. Hammarfjord O, Wallin RP. Dendritic cell function at low physiological temperature. J Leukoc Biol 2010; 88:747–756.
28. Chieppa M, Rescigno M, Huang AY, Germain RN. Dynamic imaging of dendritic cell extension into the small bowel lumen in response to epithelial cell TLR engagement. J Exp Med 2006;203:2841–2852.
29. Merad M, Manz MG. Dendritic cell homeostasis. Blood 2009;113:3418–3427.
30. Hardbower DM, Asim M, Luis PB, Singh K, Barry DP, Yang C, Steeves MA, Cleveland JL, Schneider C, Piazuelo MB, Gobert AP, Wilson KT. Ornithine decarboxylase regulates M1 macrophage activation and mucosal inflammation via histone modifications. Proc Natl Acad Sci U S A 2017;114:E751–E760.
31. Drakes ML, Czinn SJ, Blanchard TG. Regulation of murine dendritic cell immune responses by Helicobacter felis antigen. Infect Immun 2006;74:4624–4633.
32. Lamb A, Yang XD, Tsang YH, Li JD, Higashi H, Hatakeyama M, Peek RM, Blanke SR, Chen LF. Helicobacter pylori CagA activates NF-kappaB by targeting TAK1 for TRAF6-mediated Lys 63 ubiquitination. EMBO Rep 2009;10:1242–1249.
33. Lamb A, Chen LF. The many roads traveled by Helicobacter pylori to NFkappaB activation. Gut Microbes 2010;1:109–113.
34. Tran CT, Garcia M, Garnier M, Burucoa C, Bodet C. Inflammatory signaling pathways induced by Helicobacter pylori in primary human gastric epithelial cells. Innate Immun 2017;23:165–174.
35. Mustapha P, Paris I, Garcia M, Tran CT, Cremniter J, Garnier M, Faure JP, Barthes T, Boneca IG, Morel F, Lecron JC, Burucoa C, Bodet C. Chemokines and antimicrobial peptides have a cag-dependent early response to Helicobacter pylori infection in primary human gastric epithelial cells. Infect Immun 2014; 82:2881–2889.
36. Vanbervliet B, Homey B, Durand I, Massacrier C, Ait-Yahia S, de Bouteiller O, Vicari A, Caux C. Sequential involvement of CCR2 and CCR6 ligands for immature dendritic cell recruitment: possible role at inflamed epithelial surfaces. Eur J Immunol 2002;32:231–242.
37. Dieu MC, Vanbervliet B, Vicari A, Bridon JM, Oldham E, Ait-Yahia S, Briere F, Zlotnik A, Lebecque S, Caux C. Selective recruitment of immature and mature dendritic cells by distinct chemokines expressed in different anatomic sites. J Exp Med 1998;188:373–386.
38. Abernethy NJ, Hay JB, Kimpton WG, Washington E, Cahill RN. Lymphocyte subset-specific and tissue-specific lymphocyte-endothelial cell recognition mechanisms independently direct the recirculation of lymphocytes from blood to lymph in sheep. Immunology 1991;72:239–245.

39. Rieder G, Einsiedl W, Hatz RA, Stolte M, Enders GA, Walz A. Comparison of CXC chemokines ENA-78 and interleukin-8 expression in Helicobacter pylori-associated gastritis. Infect Immun 2001;69:81–88.
40. Veinotte L, Gebremeskel S, Johnston B. CXCL16-positive dendritic cells enhance invariant natural killer T cell-dependent IFNgamma production and tumor control. Oncoimmunology 2016;5:e1160979.
41. Binti Mohd Amir NAS, Mackenzie AE, Jenkins L, Boustani K, Hillier MC, Tsuchiya T, Milligan G, Pease JE. Evidence for the existence of a CXCL17 receptor distinct from GPR35. J Immunol 2018;201:714–724.
42. Cavarelli M, Foglieni C, Rescigno M, Scarlatti G. R5 HIV-1 envelope attracts dendritic cells to cross the human intestinal epithelium and sample luminal virions via engagement of the CCR5. EMBO Mol Med 2013; 5:776–794.
43. Yin Y, Qin T, Wang X, Lin J, Yu Q, Yang Q. CpG DNA assists the whole inactivated H9N2 influenza virus in crossing the intestinal epithelial barriers via trans-epithelial uptake of dendritic cell dendrites. Mucosal Immunol 2015;8:799–814.
44. Martin-Latil S, Gnadig NF, Mallet A, Desdouits M, Guivel-Benhassine F, Jeannin P, Prevost MC, Schwartz O, Gessain A, Ozden S, Ceccaldi PE. Transcytosis of HTLV-1 across a tight human epithelial barrier and infection of subepithelial dendritic cells. Blood 2012;120:572–580.
45. Sebrell TA, Sidar B, Bruns R, Wilkinson RA, Wiedenheft B, Taylor PJ, Perrino BA, Samuelson LC, Wilking JN, Bimczok D. Live imaging analysis of human gastric epithelial spheroids reveals spontaneous rupture, rotation and fusion events. Cell Tissue Res 2018; 371:293–307.
46. Bimczok D, Grams JM, Stahl RD, Waites KB, Smythies LE, Smith PD. Stromal regulation of human gastric dendritic cells restricts the Th1 response to Helicobacter pylori. Gastroenterology 2011; 141:929–938.
47. Roe MM, Swain S, Sebrell TA, Sewell MA, Collins MM, Perrino BA, Smith PD, Smythies LE, Bimczok D. Differential regulation of CD103 (alphaE integrin) expression in human dendritic cells by retinoic acid and Toll-like receptor ligands. J Leukoc Biol 2017; 101:1169–1180.
48. Schneider CA, Rasband WS, Eliceiri KW. NIH Image to ImageJ: 25 years of image analysis. Nat Methods 2012; 9:671–675.
49. Nookaew I, Thorell K, Worah K, Wang S, Hibberd ML, Sjovall H, Pettersson S, Nielsen J, Lundin SB. Transcriptome signatures in Helicobacter pylori-infected mucosa identifies acidic mammalian chitinase loss as a corpus atrophy marker. BMC Med Genomics 2013;6:41.

Received August 15, 2017. Accepted February 20, 2019.

Correspondence
Address correspondence to: Diane Bimczok, DVM, PhD, Department of Microbiology and Immunology, Montana State University, 2155 Analysis Drive, Bozeman, Montana 59717. e-mail: diane.bimczok@montana.edu; fax: (406) 994-3953.

Acknowledgments
The authors would like to thank Dr Ellen Lauchnor (MSU Department of Biological Engineering) for performing oxygen measurements in the spheroids, Dr Paul Harris (Pontifical Catholic University of Chile, Santiago, Chile) for providing human gastric tissue microarrays, and Thea Sherwood for helping with MoDC preparation.

Author contributions
Thomas A. Sebrell, Marziah Hashimi, Royce Wilkinson, Liliya Kirpotina, Diane Bimczok, and Barkan Sidar designed and performed the experiments; Diane Bimczok and James N. Wilking supervised the experimental work; Paul J. Taylor designed and provided the EmbryoCradle microinjector; Marziah Hashimi, Zeynep Malkoç, Thomas A. Sebrell, and Diane Bimczok analyzed the data; Diane Bimczok, Thomas A. Sebrell, Mark Quinn, and Marziah Hashimi wrote and edited the manuscript; and Diane Bimczok, James N. Wilking, Mark Quinn, and Paul J. Taylor provided funding for the study. All authors have reviewed and agree with the manuscript content.

Conflicts of interest
This author discloses the following: Paul Taylor is the owner of GeneSearch, Inc (Bozeman, MT), which manufactures the EmbryoCradle microinjector that was used in this study. The remaining authors disclose no conflicts. The funding agencies played no role in the study design, collection, analysis, or interpretation of data.

Funding
Supported by by National Institutes of Health grants K01 DK097144 and R03 DK107960 (D.B.), the National Science Foundation grant DMR-1455247 (J.N.W.), and the Montana University System Research Initiative 51040-MUSRI2015-03 (D.B.). Also supported by the National Institutes of Health Institutional Development Award (IDeA) Program grant P30 GM110732 (D.B., M.T.Q.). GeneSearch, Inc, development of the GeneSearch Embryo Cradle was funded by a Small Business Innovation Research (SBIR) grant from Office of Research Infrastructure Programs (ORIP)/National Institutes of Health R44 OD012083 (P.J.T.).

Supplementary Table 1. Raw Data Chemokine Array of *H pylori*–Infected Gastric Organoids

	EXPERIMENT 1			EXPERIMENT 2			EXPERIMENT 3			EXPERIMENT 4		
TARGET	Control	*H pylori*	*P* value	Control	*H pylori*	*P* value	Control	*H pylori*	*P* value	Control	*H pylori*	*P* value
CCL1	0.82	1.90	**<.001**	0.8	0.8	.855	0.65	0.43	**.028**	0.37	0.23	**.032**
CCL14	1.28	1.96	**.001**	1.0	0.8	.487	0.75	0.43	.137	0.40	0.21	**.025**
CCL15	0.36	0.86	**.010**	0.9	1.5	**.020**	0.64	0.66	.832	0.31	0.20	**.012**
CCL17	1.60	1.54	.784	1.0	0.9	.837	0.74	0.84	.143	0.46	0.29	**.007**
CCL18	1.12	1.61	**.011**	0.8	0.7	.657	0.73	0.39	**.004**	0.36	0.22	**.002**
CCL19	0.81	0.68	.481	0.8	1.1	.214	0.48	0.64	**.037**	0.43	0.30	.071
CCL2	1.61	2.74	**<.001**	1.0	1.5	**.035**	0.52	0.61	.343	0.30	0.22	**.023**
CCL20	1.44	3.47	**<.001**	5.3	9.5	**<.001**	1.40	5.73	**.001**	1.43	7.85	**.001**
CCL21	0.58	0.75	.391	0.7	0.7	.852	0.55	0.48	.426	0.37	0.22	**.016**
CCL22	1.14	0.96	.350	0.8	0.8	.906	0.57	0.37	**.024**	0.44	0.25	**.017**
CCL26	0.71	1.14	**.027**	1.1	1.2	.860	1.21	1.02	.584	0.53	0.30	**.000**
CCL28	2.22	2.51	.121	1.0	0.8	.448	1.02	0.87	.733	0.49	0.31	**.024**
CCL3/CCL4	1.50	1.70	.290	0.9	0.9	.902	0.72	0.83	.286	0.31	0.19	**.004**
CCL5	1.00	1.22	.258	0.8	0.6	.591	0.57	0.69	**.024**	0.31	0.22	**.011**
CCL7	0.88	1.22	.083	0.8	0.7	.528	0.60	0.49	.418	0.34	0.19	**.007**
CHEMERIN	1.57	1.53	.827	1.0	0.8	.489	0.79	0.74	**.010**	0.49	0.30	**.037**
CX3CL1	1.65	1.91	.176	0.9	1.0	.629	0.72	0.85	.194	0.36	0.29	.215
CXCL1	2.03	3.65	**<.001**	4.2	6.6	**<.001**	2.40	5.08	**.003**	4.09	4.56	.297
CXCL10	0.87	0.85	.957	1.3	1.9	**.025**	1.34	0.94	**.001**	0.71	0.52	**.002**
CXCL11	1.60	1.75	.432	1.0	1.1	.552	0.59	0.80	.060	0.35	0.23	**.009**
CXCL12	0.20	0.21	.959	1.1	1.1	.886	0.80	0.81	.701	0.63	0.41	**.002**
CXCL16	1.87	2.74	**<.001**	4.5	3.6	**<.001**	2.57	1.81	**.004**	3.56	1.88	**.001**
CXCL17	2.34	2.26	.697	6.7	5.6	**<.001**	4.52	3.13	**.004**	6.45	1.84	**.000**
CXCL4	1.08	1.21	.514	1.3	1.2	.540	2.05	0.59	**.002**	1.83	0.92	**.002**
CXCL5	4.96	4.91	.800	9.8	12.1	**<.001**	5.17	4.92	.095	0.32	0.22	**.033**
CXCL7	0.76	1.97	**<.001**	2.3	1.9	.089	1.24	1.19	.841	0.58	0.81	**.001**
CXCL8	1.62	3.99	**<.001**	5.1	7.1	**<.001**	3.60	3.61	.995	4.20	6.44	**.015**
CXCL9	1.54	2.11	.004	1.0	1.0	.887	0.94	1.04	.624	0.44	0.31	**.048**
IL16	1.57	1.45	.515	0.9	0.9	.888	0.90	0.82	.704	0.36	0.27	.134
MIDKINE	1.66	2.14	.015	2.9	2.2	**.004**	3.74	0.93	**.011**	1.84	1.04	**.003**
XCL1	1.51	1.80	.126	1.0	1.3	.325	0.60	0.90	**.001**	0.39	0.35	.096

NOTE. Chemokine detection in gastric spheroid supernatants analyzed using the Proteome Profiler Human Chemokine Array Kit. Relative protein concentrations in supernatants collected after 48 hours of culture from noninfected and *H pylori*–infected gastric spheroids compared with background levels present in spheroid culture medium was determined by densitometry. Data sets from 2 independent experiments are shown. *P* values were calculated using a Student *t* test and were considered significant at $P \leq .05$ (values bolded).

Supplementary Table 2. Raw Data PCR Array of *H pylori*–Infected Gastric Organoids

Target	Untreated			*H pylori*–infected			*P* value	Significant?
C5	1.0	1.0	1.0	1.0	0.9	1.2	.7247	
C5AR1	1.0	1.0	1.0	10.3	1.3	0.1	.4185	
ACKR2	1.0	1.0	1.0	10.2	1.8	15.9	.1126	
CCL1	1.0	1.0	1.0	1.4	2.0	0.9	.2446	
CCL11	1.0	1.0	1.0	1.0	0.0	1.2	.5122	
CCL13	1.0	1.0	1.0	1.0	0.0	2.6	.8047	
CCL14	1.0	1.0	1.0	0.1	0.6	1.1	.2381	
CCL15	1.0	1.0	1.0	0.6	1.0	92.4	.3767	
CCL16	1.0	1.0	1.0	0.5	2.0	2.2	.3504	
CCL17	1.0	1.0	1.0	2.1	1.9	22.5	.3156	
CCL18	1.0	1.0	1.0	21.2	0.0	1.2	.4002	
CCL19	1.0	1.0	1.0	0.1	0.7	0.1	.0249	Down*
CCL2	1.0	1.0	1.0	2.6	8.0	17.5	.1271	
CCL20	1.0	1.0	1.0	20.9	15.8	48.2	.0533	
CCL21	1.0	1.0	1.0	0.0	1.1	1.2	.5766	
CCL22	1.0	1.0	1.0	301.3	0.6	120.3	.1851	
CCL23	1.0	1.0	1.0	0.9	0.3	16.9	.4069	
CCL24	1.0	1.0	1.0	108.0	0.1	0.1	.3848	
CCL25	1.0	1.0	1.0	32.6	0.3	0.6	.3965	
CCL26	1.0	1.0	1.0	1.7	0.8	0.8	.7556	
CCL27	1.0	1.0	1.0	1.3	0.8	0.1	.4862	
CCL28	1.0	1.0	1.0	0.8	1.2	0.4	.4353	
CCL3	1.0	1.0	1.0	13.7	0.9	1.2	.3689	
CCL4	1.0	1.0	1.0	61.6	0.0	1.2	.3825	
CCL5	1.0	1.0	1.0	30.4	0.7	23.8	.1271	
CCL7	1.0	1.0	1.0	1.3	10.2	1.5	.3193	
CCL8	1.0	1.0	1.0	1.0	0.2	1.2	.5484	
CCR1	1.0	1.0	1.0	1.4	0.4	0.3	.4411	
CCR10	1.0	1.0	1.0	0.5	0.3	1.2	.2889	
CCR2	1.0	1.0	1.0	1.1	0.7	10.6	.3877	
CCR3	1.0	1.0	1.0	2.7	0.7	0.4	.7306	
CCR4	1.0	1.0	1.0	1.0	0.6	1.2	.7247	
CCR5	1.0	1.0	1.0	1.0	0.0	1.2	.5122	
CCR6	1.0	1.0	1.0	6.3	1.9	1.2	.2523	
CCR7	1.0	1.0	1.0	26.1	1.5	1.2	.3561	
CCR8	1.0	1.0	1.0	6.3	1.4	3.4	.1305	
CCR9	1.0	1.0	1.0	2.6	0.6	0.8	.6279	
ACKR4	1.0	1.0	1.0	1.1	1.4	1.2	.0572	
CCRL2	1.0	1.0	1.0	2.1	1.9	2.2	.0003	Up***
CKLF	1.0	1.0	1.0	1.0	1.3	0.8	.8298	
CMKLR1	1.0	1.0	1.0	1.0	27.0	1.2	.3690	
CMTM1	1.0	1.0	1.0	1.3	1.3	0.6	.7893	
CMTM2	1.0	1.0	1.0	1.8	0.5	0.4	.8354	
CMTM3	1.0	1.0	1.0	3.7	0.8	0.5	.5492	
CMTM4	1.0	1.0	1.0	1.6	1.1	0.6	.7465	
CX3CL1	1.0	1.0	1.0	9.5	1.0	35.3	.2387	
CX3CR1	1.0	1.0	1.0	1.0	0.9	1.2	.7247	
CXCL1	1.0	1.0	1.0	17.3	12.3	29.0	.0200	Up*
CXCL10	1.0	1.0	1.0	99.4	1.2	8.5	.3255	
CXCL11	1.0	1.0	1.0	211.6	0.9	0.0	.3773	

Supplementary Table 2. Continued

Target	Untreated			*H pylori*–infected			*P* value	Significant?
CXCL12	1.0	1.0	1.0	4.4	0.8	1.2	.3761	
CXCL13	1.0	1.0	1.0	3.6	1.5	2.6	.0611	
CXCL14	1.0	1.0	1.0	1.0	0.9	32.9	.3759	
CXCL16	1.0	1.0	1.0	1.7	1.4	1.1	.0821	
CXCL2	1.0	1.0	1.0	10.2	7.2	14.5	.0104	Up*
CXCL3	1.0	1.0	1.0	5.1	3.0	13.7	.1281	
CXCL5	1.0	1.0	1.0	1.8	1.5	7.2	.2484	
CXCL6	1.0	1.0	1.0	12.3	2.8	13.3	.0646	
CXCL9	1.0	1.0	1.0	1.5	0.9	1.9	.2102	
CXCR1	1.0	1.0	1.0	1.0	0.9	1.2	.7247	
CXCR2	1.0	1.0	1.0	0.9	0.4	0.7	.0835	
CXCR3	1.0	1.0	1.0	1.5	1.0	0.8	.6560	
CXCR4	1.0	1.0	1.0	6.3	2.1	2.5	.1205	
CXCR5	1.0	1.0	1.0	2.9	2.8	1.2	.0776	
CXCR6	1.0	1.0	1.0	1.1	0.8	1.1	1.0000	
ACKR3	1.0	1.0	1.0	1.0	0.9	1.2	.7247	
ACKR1	1.0	1.0	1.0	1.0	0.9	1.2	.7247	
FPR1	1.0	1.0	1.0	50.4	0.0	1.2	.3845	
GPR17	1.0	1.0	1.0	1.5	0.6	0.1	.5505	
HIF1A	1.0	1.0	1.0	1.7	1.4	0.9	.2263	
IL16	1.0	1.0	1.0	1.0	0.9	1.2	.7247	
IL1B	1.0	1.0	1.0	10.7	4.8	1.9	.1374	
IL4	1.0	1.0	1.0	54.4	3.4	1.2	.3432	
CXCL8	1.0	1.0	1.0	32.1	27.2	7.2	.0499	Up*
PF4V1	1.0	1.0	1.0	0.3	0.7	1.1	.2638	
PPBP	1.0	1.0	1.0	0.2	0.7	0.8	.0798	
SLIT2	1.0	1.0	1.0	1.0	0.9	1.2	.7247	
TLR2	1.0	1.0	1.0	2.9	1.7	8.1	.1751	
TLR4	1.0	1.0	1.0	2.4	1.6	1.5	.0430	
TNF	1.0	1.0	1.0	40.1	39.3	226.0	.1799	
TYMP	1.0	1.0	1.0	1.4	0.5	1.2	.9087	
XCL1	1.0	1.0	1.0	1.0	0.9	1.2	.7247	
XCL2	1.0	1.0	1.0	1.0	0.1	0.1	.1161	
XCR1	1.0	1.0	1.0	0.1	0.5	1.2	.2813	
C5	1.0	1.0	1.0	1.0	0.9	1.2	.7247	

NOTE. Relative gene expression of *H pylori*–infected gastric organoids determined by PCR array analysis. Data from 3 independent experiments are shown. *P* values were calculated using a paired Student *t* test and were considered significant at $P \leq .05$. $^{*}P \leq .05$, $^{***}P \leq .001$.
TNF, tumor necrosis factor.